# Supporting Information

## Komatsu *et al.* 10.1073/pnas.0811556106

### SI Materials and Methods

**Antibodies, Reagents, and Medium.** The following mAbs were purchased from BD Bioscience (San Jose, CA) or eBioscience (San Diego, CA): functional grade purified mAbs for CD3ε (145–2C11) and CD28 (37.51); biotin-, FITC-, PE-, PerCP-Cy5- or allophycocyanin-labeled mAbs for human CD2 (hCD2) (RPA-2.10), CD4 (RM4–5), CD25 (PC61 or 7D4), CD45.1 (A20), CD45.2 (104), CTLA-4 (UC10–4F10–11), GITR (DTA-1), TCR-β (H57–597), Vα2 (B20.1), Vβ3 (KJ25), Vβ4 (KT4), Vβ5.1/5.2 (MR9–4), Vβ6 (RR4–7), Vβ8.1/8.2 (MR5–2), Vβ14 (14–2), IFN-γ (XMG1.2), IL-2 (JES6–5H4), IL-4 (11B11), and IL-17A (eBio17B7). Anti-TGF-β1/2/3 mAbs (1D11), recombinant mouse (rm) TGFβRII-Fc chimeric proteins, rmIL-2 and recombinant human TGF-β1 were purchased from R&D systems (Minneapolis, MN), and rmIL-4, rmIL-6, rmIL-12 were obtained from PeproTech (London, UK). T cells were cultured in RPMI10 medium; RPMI-1640 supplemented with 10% fetal bovine serum, 10 mmol/L HEPES, 1 mmol/L sodium pyruvate, 50 μmol/L 2-ME, 100 U/ml penicillin, and 100 μg/ml streptomycin.

**Cell Sorting.** To purify peripheral $CD4^+$ T cell subsets, pooled spleen and lymph node (LN) cells were first depleted of $B220^+$, $CD8^+$, $CD11b^+$, $Gr1^+$, and adherent cells by panning, stained with fluorescent mAbs, and sorted on a FACSAria cell sorter. To sort $CD4^+Foxp3^+CD25^{high}$ and $CD25^-$ T cells, $Foxp3^{hCD2+}$ T cells were first enriched using the MACS system. In brief, enriched $CD4^+$ T cells were stained with FITC-anti-CD4, PE-anti-hCD2, and biotin-anti-CD25 followed by streptavidin-PE-Cy5, labeled with anti-PE microbeads, and passed through LS columns (Miltenyi Biotec) to obtain $hCD2^+$ cells, which were further FACS sorted into $CD4^+Foxp3^{hCD2+}CD25^{high}$ and $CD25^-$ T cells.

**CFSE Labeling.** Sorted T cells were incubated with 5 μmol/L (for in vitro suppression assay) or 10 μmol/L (for adoptive transfer) CFSE in PBS containing 0.1% bovine serum albumin for 10 minutes at 37 °C. The reaction was stopped by adding ×10 volume of RPMI10 medium, and cells were washed four times with RPMI10 medium.

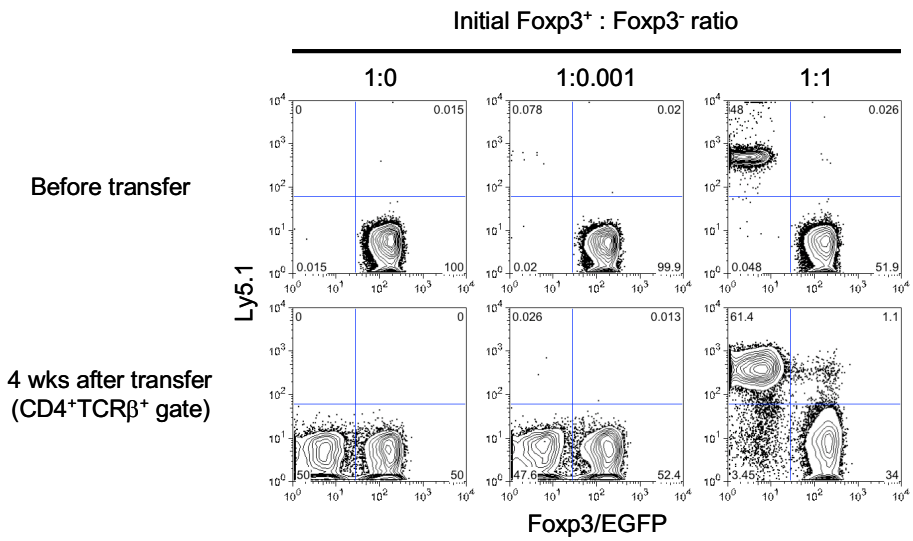


**Fig. S1.** The generation of Foxp3$^-$ T cells from Foxp3$^+$ T cells is not caused by outgrowth of Foxp3$^-$ T cells contaminating the injected donor cells, but reflects loss of Foxp3 expression in Foxp3$^+$ T cells. CD4$^+$EGFP$^+$ T cells sorted from Foxp3$^{EGFP}$ Ly5.2 mice were mixed with CD4$^+$EGFP$^-$ T cells sorted from Foxp3$^{EGFP}$ Ly5.1 mice at the indicated ratio and adoptively transferred into RAG2$^{-/-}$ host mice as described in Fig. 1*A*. Upper panels depict Ly5.1 and EGFP expression profiles of the injected populations. Lower panels show Ly5.1 and EGFP expression on LN CD4$^+$TCR$\beta^+$ cells analyzed 4 weeks after transfer.

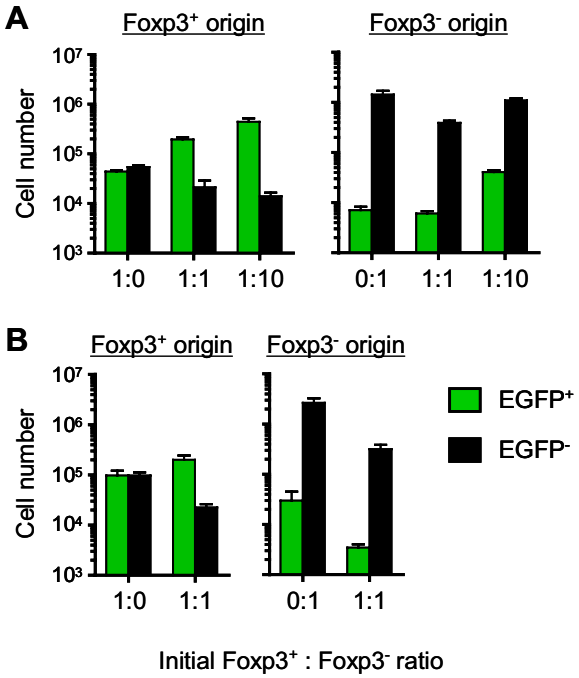


**Fig. S2.** Foxp3 down-regulation in RAG2$^{-/-}$ and CD3$\varepsilon^{-/-}$ recipients. Sorted CD4$^{+}$Foxp3/EGFP$^{+}$ and EGFP$^{-}$ T cells were injected into RAG2$^{-/-}$ (*A*) or CD3$\varepsilon^{-/-}$ mice (*B*) as described in Fig. 1*A*. Four weeks after transfer, LN and spleen (not depicted) cells were counted and stained for CD4, TCR$\beta$, and Ly5.1. Absolute numbers of Foxp3$^{+}$ (*left*) or Foxp3$^{-}$ (*right*) donor-derived T cells with the indicated EGFP phenotype are shown ($n$ = 4–5 per group).

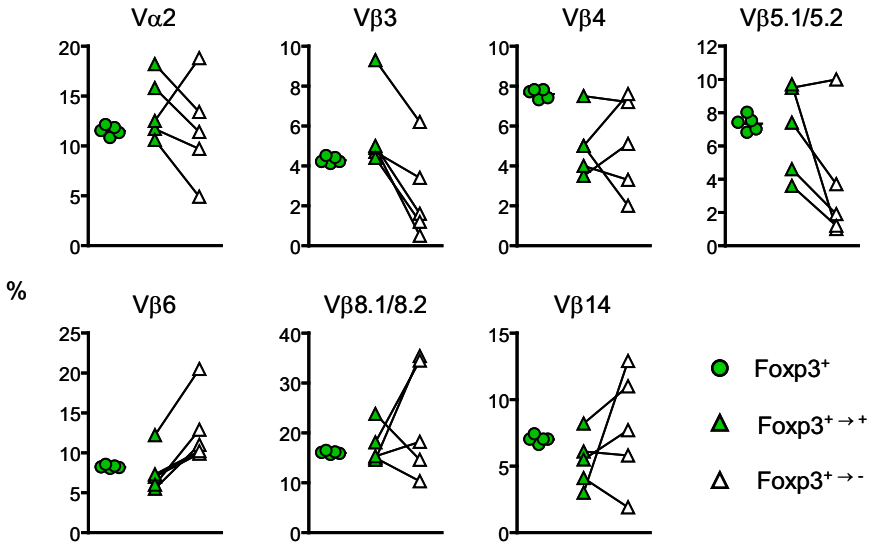


**Fig. S3.** TCR repertoires of Foxp3-maintaining and Foxp3-down-regulated T cells. $CD4^+EGFP^+$ T cells sorted from $Foxp3^{EGFP}$ Ly5.1 mice were injected into $CD3\varepsilon^{-/-}$ host mice ($1 \times 10^5$). Four weeks after transfer, LN and spleen cells from individual host mice were pooled, enriched for donor T cells by depleting $B220^+$, $CD8^+$, $CD11b^+$, and $Gr1^+$ cells by panning, and stained for Ly5.1 and the indicated TCR V$\alpha$ or V$\beta$ chains. Frequencies of cells expressing each V$\alpha$/V$\beta$ chain among the $Foxp3^{+\rightarrow+}$ and $Foxp3^{+\rightarrow-}$ cells as well as $CD4^+EGFP^+$ T cells from $Foxp3^{EGFP}$ mice were determined ($n = 5$ per group). Lines connect $Foxp3^{+\rightarrow+}$ and $Foxp3^{+\rightarrow-}$ cells from each individual host.

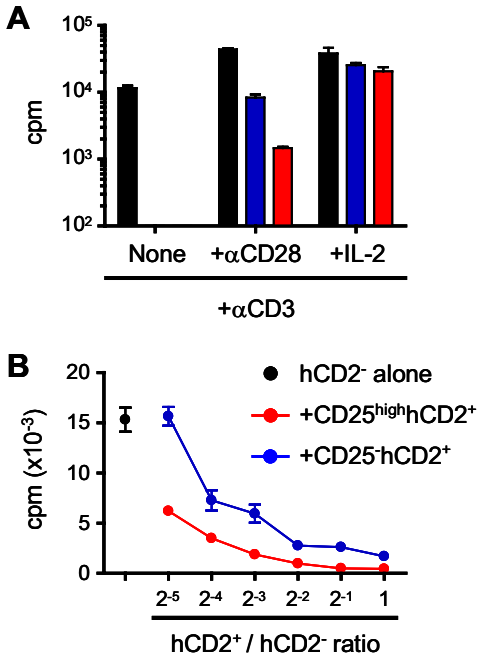


**Fig. S4.** The capacity for anergy and suppression in CD25$^{-}$ and CD25$^{high}$ subsets of CD4$^{+}$Foxp3$^{+}$ T cells. (*A*) Sorted CD4$^{+}$Foxp3$^{hCD2-}$ (black bar), CD4$^{+}$Foxp3$^{hCD2+}$CD25$^{high}$ (red bar), CD4$^{+}$Foxp3$^{hCD2+}$CD25$^{-}$ (blue bar) T cells were stimulated with anti-CD3 mAbs and splenic APCs in the presence or absence of IL-2 or anti-CD28 mAbs. (*B*) Sorted CD4$^{+}$Foxp3$^{hCD2-}$ T cells ($2 \times 10^4$/well) were stimulated with anti-CD3 mAbs and splenic APCs ($8 \times 10^4$/well) in the presence or absence of titrated numbers of CD4$^{+}$Foxp3$^{hCD2+}$CD25$^{high}$ or CD25$^{-}$ T cells. On day 3, [$^3$H]thymidine (1 $\mu$Ci/well) was added during the last 6 hours of culture. Results are shown as mean [$^3$H]thymidine incorporation $\pm$ SD. in triplicate cultures.